PHYSICAL REVIEW C VOLUME 23, NUMBER 2 FEBRUARY 1981

Two-nucleon processes in a coupled-channel approach to pion-nucleus single-charge-exchange reactions

L. C. Liu
Los Alamos Scientific Laboratory, University of California, Los Alamos, New Mexico 87545
(Received 17 July 1980)

A momentum space coupled-channel formalism is proposed for the study of pion-nucleus single-charge-exchange reactions at medium energies. Formal elimination of certain reaction channels leads to a reduced set of coupled equations with a complex and energy-dependent interaction. A nonperturbative method based upon unitarity considerations is then used to construct each order of this effective pion-nucleus interaction. Our analysis thus leads to a second-order pion-nucleus interaction with analytical properties very different from those obtained from multiple-scattering theory. The theory is applied to the study of pion-^{13}C elastic scattering and the single-charge-exchange reaction $^{13}C(\pi^+,\pi^0)^{13}N$(g.s.). Included in our calculations are the first- and second-order pion-nucleus strong interactions, and the pion-nucleus Coulomb interaction. We have calculated the first-order interaction using a covariant, nonstatic theory and have evaluated contributions to the second-order interaction arising from two-nucleon processes related to true pion absorption and to the scattering of pions from a nucleon pair. We present a general relation connecting the second-order pion-nucleus strong interaction potentials of nuclei whose structure do not differ appreciably. Theoretical results for π^{13}C elastic scattering predicted by our theory are found to be in good agreement with the data. The calculated excitation function of the single-charge-exchange reaction exhibits a high sensitivity to the type of two-nucleon processes considered. Pion-nucleus single-charge-exchange reactions therefore have promise as a tool for investigating pion-nucleus reaction mechanisms.

[NUCLEAR REACTIONS Coupled-channel theory, pion-nucleus single-charge-exchange reactions, pion absorption, nucleon-nucleon correlations, π^{13}C elastic cross sections at 50 and 180 MeV, excitation function of $^{13}C(\pi^+,\pi^0)^{13}N$(g.s.) between 30 and 260 MeV.]

I. INTRODUCTION

Pion-nucleus charge exchange reactions have received considerable attention in recent years. A large number of experimental and theoretical works have been published.[1,2] In this work, we will discuss a new approach to charge exchange reactions which has not been explored previously. That is, we propose the use of single charge exchange (SCE) reactions to study the nature of the second-order pion-nucleus optical potential. As we know, the second-order optical potential plays an important role in the description of pion-nucleus elastic scattering.[3-5] In the past we have carried out a systematic study of pion elastic scattering from light and medium-mass nuclei at pion energies between 30 and 340 MeV (Refs. 3 and 4) using a covariant scattering theory.[6] The microscopic first-order optical potential used in our analysis is parameter-free and is constructed by performing a complete integration over the Fermi motion of the target nucleons. The off-shell effects related to nuclear binding have also been treated carefully.[7] On the basis of this rather accurate first-order theory, we have parametrized the second-order potential and determined the parameters by performing a chi-square fit to the experimental differential cross sections.[4] The second-order optical potential is closely related to reaction mechanisms involving two-nucleon processes. At pion energies below 300 MeV, the leading two-nucleon processes are true pion absorption by two nucleons and pion scattering from a correlated pair of nucleons. (Both these reaction mechanisms lead to a density-square dependence of the optical potential.) Consequently, it is important to obtain information as to the relative strength of these two competitive mechanisms. We will show that the SCE reactions leading to isobaric analog states (IAS) are very sensitive to these types of two-nucleon processes. As an application of our theory, we will study the excitation function of the $^{13}C(\pi^+,\pi^0)^{13}N$ (g.s.) reaction and the differential cross sections for π^{13}C elastic scattering, making use of our knowledge of the pion-^{12}C second-order optical potential.[4] The good agreement between theoretical results and the experimental π^{13}C elastic scattering data (see Sec. IV) is particularly encouraging in that no new parameter has been introduced in the present calculation.

The experimental results for the $^{13}C(\pi^+,\pi^0)^{13}N$ (g.s.) reaction have evoked a great deal of interest. Activation measurements by Shamai *et al.*[8] at pion energies between 70 and 230 MeV, and measurements by Zaider *et al.*[9] at 30 to 90 MeV show an almost energy-independent cross sec-

tion of ~1 mb. However, in the (3,3) resonance region, most theoretical calculations give results lower than the experimental data of Ref. 8 by almost a factor of 2.[10-12] In addition, theoretical excitation functions exhibit a minimum in this region.[13] Recently, it has been suggested[14,15] that pion-nucleon scattering amplitudes used in the calculation of the SCE reaction should be evaluated at different energies for different isospin channels so as to take into account the difference between the binding of neutrons and protons in the nucleus. While calculations[14,16] in which this energy-difference was treated as a free parameter did provide a fit to the activation data of Ref. 8, preliminary results based upon a careful microscopic calculation[17] indicate that the effect on the SCE reaction due to a realistic consideration of the energy-difference is very small. In an earlier study Anderson *et al.*[18] had reexamined some experimental aspects of the activation measurements and had estimated target thickness effects (due to secondary particle reactions) on the measured cross sections. Their calculations indicate that lower cross section values may be obtained when the cross sections due to secondary particle reactions are subtracted from these activation measurements. Bowman *et al.* have made an exponential fit to the preliminary $^{13}C(\pi^+, \pi^0)^{13}N$(g.s.) angular distribution at 150 MeV, measured with the LAMPF π^0 spectrometer.[19] They have also obtained an estimated integrated cross section which is considerably lower than the one reported in Ref. 8. Clearly, further experimental and theoretical studies are necessary for providing a final answer as to the magnitude and the energy-dependence of the cross section of this SCE reaction.[20]

In the present analysis we have assumed isospin-symmetry for the pion-nucleus strong interaction. However, we have also taken into account the macroscopic isospin symmetry breaking due to the pion-nucleus Coulomb interaction. Our analysis makes use of a momentum-space coupled-channel formalism. The basic theory is developed in Sec. II. One important feature of our analysis is the use of a complex and energy-dependent pion-nucleus interaction derived from considerations based on unitarity.[21] The consistency of the theory is achieved through the use of a common interaction to describe both elastic scattering and SCE reaction phenomena. For example, the first- and second-order potentials responsible for the SCE reactions are connected in a definitive way to the first- and second-order optical potentials for elastic scattering.

Several calculations reported in literature considered effects of second-order interactions on SCE reactions. Warzawski *et al.* calculated contributions due to isovector nucleon-nucleon correlations in the framework of the distorted-wave impulse approximation (DWIA).[22] In that calculation the distorted waves were generated, however, only with the first-order optical potential. Omission of the attenuation of the pion flux due to the second-order optical potential will necessarily yield higher calculated SCE cross sections. The approximation in that work is, therefore, not consistent in the treatment of the second-order interaction (see a discussion in Sec. IV). In Ref. 16, a phenomenological second-order optical potential was added to a first-order optical potential to generate distorted waves. Then the second-order direct interaction of Ref. 22 was included in the calculations. It is very likely that the direct interaction part of the second-order potential so introduced cannot be related to the phenomenological optical potential used in the same work, in the sense that they do not derive from a common interaction. Other theoretical works have considered correlation effects using a perturbative approach to describe the basic interaction due to two-nucleon mechanisms (see Sec. II). However, the question of true pion absorption as related to two-nucleon processes has not been addressed.

In Sec. III we show how, by isospin analysis, one can determine the second-order potentials for $\pi^{13}C$ systems from the knowledge of the $\pi^{12}C$ second-order optical potential. We will also discuss the sensitivity of the SCE reaction to the type of two-nucleon reaction mechansims being considered. Theoretical results and the discussion of these results will be given in Sec. IV.

II. BASIC THEORY

In this section we develop a coupled-channel formalism suitable to the study of SCE reactions leading to IAS. Central to the analysis presented here is the use of a nonperturbative approach to derive the effective pion-nucleus interaction. Thus the analytical properties of the second-order pion-nucleus interaction that emerges from this analysis are very different from those obtained from multiple-scattering theory.

We divide the complete Hilbert space into three orthogonal subspaces. Let P_a project onto the channel describing the elastic scattering of incoming charged pions by the target nucleus, and P_b onto the channel which describes the elastic scattering of charge-exchanged pions by the isobaric analong nucleus. Let P_x be the pro-

jector which projects onto all other reaction channels. It follows by construction that $P_a+P_b+P_x=1$ and $P_iP_j=\delta_{ij}P_j$ $(i,j=a,b,x)$. We also define the total wave function Ψ, and various channel wave functions, Ψ_i, through the relations:

$$H|\Psi\rangle=E|\Psi\rangle \tag{2.1}$$

and

$$P_i|\Psi\rangle=|\psi_i\rangle,\quad i=a,b,x. \tag{2.2}$$

In Eq. (2.1) $H=K+U$. Here the K and U represent, respectively, the kinetic energy operator and the interaction between the pion and the nucleus. Using standard projector algebra, we can rewrite Eq. (2.1) as:

$$(E-K-U_{aa})|\psi_a\rangle=U_{ab}|\psi_b\rangle+U_{ax}|\psi_x\rangle, \tag{2.3}$$

$$(E-K-U_{bb})|\psi_b\rangle=U_{bx}|\psi_x\rangle+U_{ba}|\psi_a\rangle, \tag{2.4}$$

and

$$(E-K-U_{xx})|\psi_x\rangle=U_{xa}|\psi_a\rangle+U_{xb}|\psi_b\rangle, \tag{2.5}$$

where $U_{ij}=P_iUP_j$ $(i,j=a,b,x)$. Upon eliminating $|\psi_x\rangle$ from these equations, we obtain a system of two coupled equations:

$$(E-K-\tilde{U}_{aa})|\psi_a\rangle=\tilde{U}_{ab}|\psi_b\rangle, \tag{2.6}$$

$$(E-K-\tilde{U}_{bb})|\psi_b\rangle=\tilde{U}_{ba}|\psi_a\rangle. \tag{2.7}$$

Here $\tilde{U}_{ij}=P_i\tilde{U}P_j$ $(i,j=a,b)$ are the matrix elements of an effective interaction $\tilde{U}$ and are defined by:

$$\tilde{U}_{aa}\equiv U_{aa}+U_{ax}G_x^{(+)}(E)U_{xa}, \tag{2.8}$$

$$\tilde{U}_{bb}\equiv U_{bb}+U_{bx}G_x^{(+)}(E)U_{xb}, \tag{2.9}$$

and

$$\tilde{U}_{ba}\equiv U_{ba}+U_{bx}G_x^{(+)}(E)U_{xa}, \tag{2.10}$$

with

$$G_x^{(+)}(E)=(E-K-U_{xx}+i\epsilon)^{-1}. \tag{2.11}$$

Similar relations hold for $\tilde{U}_{ab}$. An inspection of these equations indicates that $\tilde{U}_{aa}$ and $\tilde{U}_{bb}$ are, respectively, the pion-nucleus optical potentials in the channels a and b. On the other hand, $\tilde{U}_{ab}$ and $\tilde{U}_{ba}$ represent the single charge exchange interactions which couple the channels a and b. Equation (2.10) further suggests that $\tilde{U}$ is complex and is energy dependent. Following Ref. 21, we expand the propogator $G_x^{(+)}(E)$ in terms of a complete set of biorthonormal eigenfunctions which are solutions of the equation $(K+U_{xx})\psi_x=E_x\psi_x$, and write

$$G_x^{(+)}(E)=\int dE_x|\psi_x^{(+)}\rangle(E-E_x+i\epsilon)^{-1}\langle\bar{\psi}_x^{(+)}|. \tag{2.12}$$

Introducing Eq. (2.12) into Eqs. (2.8)–(2.10), and using the relations between the scattering wave state $|\psi_x^{(+)}\rangle$ and the plane-wave state $|x\rangle$

$$U_{bx}|\psi_x^{(+)}\rangle=T_{bx}|x\rangle \tag{2.13}$$

and

$$\langle\bar{\psi}_x^{(+)}|U_{xa}=\langle x|T_{xa}^{\dagger}, \tag{2.14}$$

we obtain

$$\tilde{U}_{aa}=U_{aa}+\int dE_xT_{ax}(E-E_x+i\epsilon)^{-1}T_{xa}^{\dagger} \tag{2.15}$$

and

$$\tilde{U}_{ba}=U_{ba}+\int dE_xT_{bx}(E-E_x+i\epsilon)^{-1}T_{xa}^{\dagger}. \tag{2.16}$$

There are similar expressions for $\tilde{U}_{bb}$. We note that the numerator of Eq. (2.15) is proportional to the product $TT^{\dagger}$ and is therefore always positive. Consequently, the imaginary part of the optical potentials, $\tilde{U}_{aa}$ and $\tilde{U}_{bb}$, is always negative, independent of the models used for T and $T^{\dagger}$. It was further shown in Ref. 21 that each optical potential can be written as an expansion classified by the number of target nucleons interacting with the projectile, and each term in the expansion has a negative imaginary part. The definitely negative sign of the imaginary part of the optical potentials in our theory is a direct result of the procedure used in obtaining Eq. (2.15). It represents the transfer of flux from the elastic channel to reaction channels as required by the unitarity. Had an iterative method been used in solving Eqs. (2.8)–(2.10), one would have obtained the usual multiple-scattering expansion of the optical potential in which the second-order optical potential is proportional to $(E-E_x+i\epsilon)^{-1}T$. The numerator of this last quantity is thus given by the product TT which, in general, does not have a definite sign. Consequently, the imaginary part of this latter second-order potential can be either positive or negative. The situation is especially serious when there is resonance in the elementary projectile-nucleon interaction. For instance, if T is replaced by the πN scattering amplitude, then $TT=(f_{\pi N})^2$. Owing to the presence of the (3,3) resonance in the pion-nucleon system, the quantity $\mathrm{Im}(f_{\pi N}f_{\pi N})$ is a rapidly varying function of the energy and can become positive. Such theories can often lead to numerical results[23] that do not have any simple physical interpretation. Consequently, in the present analysis we will only use Eqs. (2.15) and (2.16) to construct the second-order optical potentials.

We now apply our formalism to the SCE reaction $^{13}C(\pi^+,\pi^0)^{13}N(g.s.)$ and let a and b denote, respectively, the elastic channel of the π^+-^{13}C and π^0-^{13}N systems. For notational convenience in the following discussion, we write the interaction $\tilde{U}$ in an expression which does not have an apparent

matrix form:

$$\tilde{U} = V + t_\pi(\tfrac{1}{2} - t_A)V_c - (\tfrac{1}{2} + t_A)\Delta_c. \tag{2.17}$$

Equation (2.17) is equivalent to a (2×2) matrix representation of $\tilde{U}$, provided we also replace the one-column vector representation of the two-channel pion-nucleus wave function by the expansion $\Psi = \psi_a + \psi_b$. In Eq. (2.17), V is the complex and energy-dependent pion-nucleus strong interaction. The quantities t_π and t_A denote the third components of the isospin operators acting, respectively, on the pion and the nucleus. Our convention for the isospin is that the eigenvalue of t_A equals $\frac{1}{2}$ for ^{13}N and $-\frac{1}{2}$ for ^{13}C. Finally, the quantity Δ_c represents the mass difference between the two channels being considered. In the present example, $\Delta_c = m(\pi^+) + m(^{13}\mathrm{C}) - m(\pi^0) - m(^{13}\mathrm{N}) \simeq 2.4$ MeV, reflecting the Coulomb splitting of the two channels.

Since the pion has isospin one and is spinless, while either ^{13}C or ^{13}N has isospin $\frac{1}{2}$ and spin $\frac{1}{2}$, it follows that the pion-nucleus strong interaction V has the general form

$$V = W + \vec{\tau}_\pi \cdot \vec{\tau}_A U, \tag{2.18}$$

with

$$W = W_0 - i\vec{\sigma}\cdot(\vec{k}'\times\vec{k})W_s; \tag{2.19}$$

and

$$U = U_0 - i\vec{\sigma}\cdot(\vec{k}'\times\vec{k})U_s\,. \tag{2.20}$$

Here the $\vec{k}$ and $\vec{k}'$ are the unit vectors in the direction of the initial and final pion momentum calculated in the center-of-mass frame of the pion-nucleus system. Furthermore, the strong interaction V given above is diagonal in the basis formed with the eigenvectors $|LJI\rangle$. Here the quantum numbers L, J, and I stand, respectively, for the relative orbital momentum, the total angular momentum, and the total isospin of the system. However, the full interaction $\tilde{U}$ does not conserve the total isospin and is therefore not diagonal in the basis $|LJI\rangle$. This isospin symmetry breaking is due to the second and third terms in $\tilde{U}$, which are related to Coulomb interaction and do not commute with the total isospin operator $\vec{I} = \vec{\tau}_\pi + \vec{\tau}_A$.

We use the following model wave function for the effective two-channel system of Eqs. (2.15) and (2.16):

$$\Psi = \phi_a(\vec{r})\chi_a + \phi_b(\vec{r})\chi_b. \tag{2.21}$$

Here ϕ_a and ϕ_b describe the relative motion of the pion in the physical channels π^+ ^{13}C and π^0 ^{13}N. The χ_a and χ_b represent the internal wave functions and are related to the internal wave functions of definite isospin by vector coupling

$$\chi_a = \sqrt{\tfrac{1}{3}}\chi_{(3/2)} + \sqrt{\tfrac{2}{3}}\chi_{(1/2)} \tag{2.22}$$

and

$$\chi_b = \sqrt{\tfrac{2}{3}}\chi_{(3/2)} - \sqrt{\tfrac{1}{3}}\chi_{(1/2)}, \tag{2.23}$$

Consequently, the wave function Ψ can also be written as

$$\Psi = \phi_{(3/2)}\chi_{(3/2)} + \phi_{(1/2)}\chi_{(1/2)}, \tag{2.24}$$

with $\phi_{(3/2)}$ and $\phi_{(1/2)}$ describing the relative motion of the pion in the isospin channels. Introducing Eqs. (2.17)–(2.21) into Eq. (2.1) and making use of Eqs. (2.22) and (2.23), we obtain two coupled equations:

$$(E - K - W + U - V_c)|\phi_a\rangle = \sqrt{2}\,U|\phi_b\rangle\,, \tag{2.25}$$

and

$$(E - K - W + \Delta_c|\phi_b\rangle = \sqrt{2}\,U|\phi_a\rangle. \tag{2.26}$$

Equations (2.25) and (2.26) are formally identical to the Lane equations[24–26] used for the study of (p,n) reactions. If R_N is the range of the nuclear force, then the nuclear potentials vanish at $r \gtrsim R_N$. Consequently, in the external region we have two uncoupled equations:

$$(E - K - V_c)\phi_a(\vec{r}) = 0, \quad r \gtrsim R_N, \tag{2.27}$$

and

$$(E + \Delta_c - K)\phi_b(\vec{r}) = 0, \quad r \gtrsim R_N. \tag{2.28}$$

Equation (2.28) indicates that the channel energy of the physical channel π^0-^{13}N is greater than that of the physical channel π^+-^{13}C. In the external region the radial wave functions of Eqs. (2.27) and (2.28) satisfy the following boundary conditions:

$$u_a^{LJ}(r) \underset{r>R_N}{=} e^{i\delta_a^{LJ}}\cos\delta_a^{LJ}[F_L^\eta(k_a r) + \tan\delta_a^{LJ} G_L^\eta(k_a r)], \tag{2.29}$$

and

$$u_b^{LJ}(r) \underset{r>R_N}{=} \frac{1}{2i}S_{ba}^{LJ}[H_L^{(+)}(k_b r)]_{\eta=0} \tag{2.30}$$

Here the k_a and k_b are the channel wave vectors. The F_L^η and G_L^η are the regular and irregular Coulomb functions and η is the usual Coulomb parameter. Furthermore,

$$[H_L^{(+)}(k_b r)]_{\eta=0} = G_L^0(k_b r) + iF_L^0(k_b r) = (k_b r)[n_L(k_b r) + ij_L(k_b r)].$$

The δ_a and S_{ba} are the nuclear phase shifts and the scattering function in the presence of the Coulomb interaction.

The scattering problem in the internal region can be described by the short-range part $(r \leq R_N)$ of Eqs. (2.25) and (2.26),[26] where the short-range Coulomb potential is given by $V_c(r)\theta(R_N - r)$. In

our calculations, we have used $V_c(r)\theta(R_N-r) = (Z_a e^2/2R_c)(3-r^2/R_c^2)$, with the number of protons Z_a equal to 6 and the charge radius $R_c \simeq R_N$. Since the pion-nucleus strong interaction is nonlocal, it is advantageous to solve the problem in momentum space. We have transformed the internal equations into two coupled momentum space Lippmann-Schwinger type integral equations. For each given partial wave LJ we have solved the set of equations:

$$\langle k'|\mathcal{T}_{ij}^{LJ}|k\rangle = \langle k'|\mathfrak{U}_{ij}^{LJ}|k\rangle + \sum_{m=a,b} 4\pi \int k''^2 dk'' \times \langle k'|\mathfrak{U}_{im}^{LJ}|k''\rangle G_m^{0(+)}(\vec{k}''^2)\langle k''|\mathcal{T}_{mj}^{LJ}|k'\rangle, \quad (i,j=a,b). \tag{2.31}$$

Equation (2.31) may be written in matrix notation as

$$\langle k'|\mathcal{T}^{LJ}|k\rangle = \langle k'|\mathfrak{U}^{LJ}|k\rangle + 4\pi \int k''^2 dk'' \langle k'|\mathfrak{U}^{LJ}|k''\rangle G^{0(+)}(\vec{k}''^2)\langle k''|\mathcal{T}^{LJ}|k\rangle \tag{2.32}$$

with

$$\mathfrak{U}^{LJ} = \begin{pmatrix} W^{LJ} - U^{LJ} + V_c^{LJ} & \sqrt{2}\,U^{LJ} \\ \sqrt{2}\,U^{LJ} & W^{LJ} \end{pmatrix}, \tag{2.33}$$

and

$$G^{0(+)}(\vec{k}''^2) = \begin{pmatrix} E - E_\pi(\vec{k}'') - E_A(\vec{k}'') + i\epsilon & 0 \\ 0 & E + \Delta_c - E_\pi(\vec{k}'') - E_A(\vec{k}'') + i\epsilon \end{pmatrix}. \tag{2.34}$$

Here the use of the symbol $\mathfrak{U}$ for the interaction serves as a reminder that the quantity Δ_c has been separated out from the original interaction $\tilde{U}$ [see Eqs. (2.17), (2.25), and (2.26)] and was absorbed into the definition of the channel-energy of channel b [see Eq. (2.34)]. Finally the partial wave expansion of the potential W in Eqs. (2.31)–(2.33) is given by

$$W^{LJ} = \tfrac{1}{2}\int_{-1}^{+1} d\mu \left[W_0 P_L(\mu) - W_s \frac{\mu P_L(\mu) - P_{L\pm1}(\mu)}{(1-\mu^2)^{1/2}} \right]. \tag{2.35}$$

A similar expression holds for U^{LJ} and V^{LJ}. We may note, however, that since Coulomb interaction is spin independent, the partial wave expansion of the V_c does not have a term corresponding to the second term in Eq. (2.35).

If we denote the radial wave functions of the internal equations as $u_{a,s}^{LJ}$ and $u_{b,s}^{LJ}$, then $u_{a,s}^{LJ}$ has the asymptotic behavior

$$u_{a,s}^{LJ}(r) \underset{r>R_N}{=} F^{\eta=0}(k_a r) + \mathcal{T}_{aa}^{LJ}[H_L^{(+)}(k_a r)]_{\eta=0} + \mathcal{T}_{ab}^{LJ}[H_L^{(+)}(k_b r)]_{\eta=0}. \tag{2.36}$$

A similar equation holds for $u_{b,s}^{LJ}(r)$. Here the subscript s denotes that the wave functions are due only to the nuclear potentials and the short-range part of the Coulomb interaction, V_c. Consequently, in Eq. (2.36) the functions F_L and $H_L^{(+)}$ are evaluated with $\eta=0$. The quantities $\mathcal{T}_{ij}^{LJ}$ $(i,j=a,b)$ are obtained from solving numerically the set of equations (2.31) in momentum space. The phase shifts δ_a^{LJ} and the scattering function S_{ba}^{LJ} defined in Eqs. (2.29) and (2.30) are then determined from $\mathcal{T}_{ij}^{LJ}(i,j=a,b)$ by matching the "interior" wave functions $u_{a,s}^{LJ}$ and $u_{b,s}^{LJ}$ to the "exterior" wave functions u_a^{LJ} and u_b^{LJ} at $r \gtrsim R_N$. This procedure represents a generalization of the single-channel momentum space matching method of Vincent and Phatak.[27]

By solving the coupled equations, we are able to obtain with a single calculation the differential cross sections for π^+-^{13}C elastic scattering and for the SCE reaction $^{13}C(\pi^+,\pi^0)^{13}N$(g.s.). For π^--^{13}C elastic scattering, the pion-nucleus system is in a pure isospin state of isospin $\frac{3}{2}$. In this case, we do not use the coupled-channel formalism. Instead, we solve the scattering problem by using a single-channel equation $H\psi = (K + V - V_c)\psi = E\psi$, where V is the optical potential of the π^--^{13}C system. Further, the Vincent-Phatak momentum-space matching method[27] can be used without modification to determine the nuclear phase shifts in the presence of Coulomb interaction.

III. ISOSPIN ANALYSIS OF REACTION MECHANISM

In this section we discuss models used for the first- and second-order strong interaction potentials. Our emphasis is on the investigation of the dependence of SCE reactions on types of two-nucleon processes being considered. In particular, by use of isospin analysis, we formulate a scaling method which allows us to obtain the strength of the second-order SCE potential from the second-order optical potential determined in the analysis of the elastic scattering of pions from *neighboring* nuclei. For example, we show that, within a given reaction model, the second-order SCE potential for the reaction $^{13}C(\pi^+,\pi^0)^{13}N$ (g.s.) can be determined from the knowledge of the second-order optical potential of the pion-^{12}C system. As it has been discussed in Sec. I, it is

of interest to study the relative importance between contributions to the second-order optical potential due to true pion absorption by two nucleons and scattering of pions by a nucleon pair. To implement this latter study, we extend, at the end of this section, our scaling method by introducing a mixing parameter to account for the competition between these two two-nucleon processes.

We use superscripts to denote the order of interaction. Referring to Eqs. (2.18)–(2.20), we will further employ the notation $V^{(n)} = W^{(n)} + (\vec{\tau}_\pi \cdot \vec{\tau}_A) U^{(n)}$ and $W^{(n)} = W_0^{(n)} - i\vec{\sigma} \cdot (\vec{k} \times \vec{k}) W_s^{(n)}$, $(n = 1, 2)$. A similar expression will be used for $U^{(n)}$. For the first-order potential we use the microscopic, nonstatic covariant theory employed in previous works.[3,4] We write

$$V^{(1)} = V_{\text{core}}^{(1)} + V_{\text{val}}^{(1)} . \tag{3.1}$$

In Eq. (3.1) $V_{\text{core}}^{(1)}$ is the first-order potential describing the interaction between the pion and the core nucleons. For the pion-^{13}C system, the analytical expression for $V_{\text{core}}^{(1)}$ is identical to that for the pion-carbon optical potential[4,6] except that now the nuclear wave functions are determined from electron scattering data[28] for ^{13}C. (The procedure used for determining wave functions from electron scattering data can be found in Ref. 29.) The potential $V_{\text{val}}^{(1)}$ describes the interaction between the pion and the valence nucleon and can be derived by use of methods similar to those used for $V_{\text{core}}^{(1)}$. We find

$$\langle \vec{k}'; \alpha' | V_{\text{val}}^{(1)}(E) | \vec{k}; \alpha \rangle = R^{1/2}(\vec{k}') R^{1/2}(\vec{k}) \int d\vec{Q} (M_c/E_c) \langle \vec{k}', -\vec{k}' - \vec{Q}; \alpha' | f_{\pi N}(\sqrt{s}) | \vec{k}, -\vec{k} - \vec{Q}; \alpha \rangle \rho_{nlj}^{(1)}(\vec{Q}_R, \vec{Q}'_R). \tag{3.2}$$

Here, nlj are the quantum numbers specifying the orbit of the valence nucleon and $\rho_{nlj}^{(1)}$ is the corresponding nuclear form factor. For simplicity of notation, we have used α and α' to denote, respectively, the spin and isospin quantum numbers of the pion and the nucleus in the initial and final state. We note that in the present example, the isospin of the nucleus is identical to the isospin of the valence nucleon. Furthermore, $E_c = (\vec{Q}^2 + M_c^2)^{1/2}$ is the energy of the spectator core, and $\vec{Q}_R$ and $\vec{Q}'_R$ are, respectively, the momenta of the valence nucleon in the rest frame of the initial and final target nucleus. We refer to Refs. 4 and 6 for the definition of the kinematic factors, $R^{1/2}$. Finally, in Eq. (3.2), E denotes the total energy in the center-of-mass frame of the pion-nucleus system.

The nuclear binding and the Fermi motion of the target nucleons have a significant effect on the πN interaction through the determination of the energy available to the πN collision, $\sqrt{s}$.[6] Since the πN scattering amplitude is strongly energy-dependent, we have carefully distinguished the binding energy of the valence nucleon from the binding energies of the core nucleons of different orbits. Experimental separation energies and binding energies given by Hartree-Fock calculations were used in the determination of $\sqrt{s}$ for each nucleon.

In spin and isospin space, the πN amplitude is an operator and can be written as $f_{\pi N} = f_0 - \vec{\sigma} \cdot \vec{n}_c f_1 + \vec{\tau}_\pi \cdot \vec{\tau}_N (f_2 - i\vec{\sigma} \cdot \vec{n}_c f_3)$. Here $\vec{n}_c$ is the scattering vector associated with scattering of the pion from a moving target nucleon and is to be integrated in our treatment of Fermi motion. We can therefore write $V_{\text{val}}^{(1)} = \sum_i V_{i,\text{val}}^{(1)}$ $(i = 0, 1, 2, 3)$, where $V_{i,\text{val}}^{(1)}$ is obtained by substituting f_i for $f_{\pi N}$ in Eq. (3.2). It follows from Eqs. (2.18)–(2.20) and (3.1) that $W_0^{(1)} = V_{\text{core}}^{(1)} + V_{0,\text{val}}^{(1)}$, $U_0^{(1)} = V_{2,\text{val}}^{(1)}$. Further, $W_s^{(1)}$ and $U_s^{(1)}$ can be readily calculated from $V_{1,\text{val}}^{(1)}$ and $V_{3,\text{val}}^{(1)}$.

The second-order strong interaction potential $V^{(2)}$ can also be considered as being composed of two terms

$$V^{(2)} = V_{\text{core}}^{(2)} + V_{\text{val}}^{(2)} . \tag{3.3}$$

Here $V_{\text{core}}^{(2)}$ describes the interaction between the pion and two core nucleons, while $V_{\text{val}}^{(2)}$ describes two-nucleon processes involving the valence nucleon and a core nucleon. Again, $V_{\text{core}}^{(2)}$ represents a scalar interaction and $V_{\text{val}}^{(2)}$ does not. In isospin space, one can write

$$V_{\text{val}}^{(2)} = W_{\text{val}}^{(2)} + \vec{\tau}_\pi \cdot \vec{\tau}_A U_{\text{val}}^{(2)} , \tag{3.4}$$

and similarly

$$V^{(2)} = W^{(2)} + \vec{\tau}_\pi \cdot \vec{\tau}_A U^{(2)} . \tag{3.5}$$

It follows from Eqs. (3.2)–(3.5) that $W^{(2)} = V_{\text{core}}^{(2)} + W_{\text{val}}^{(2)}$ and $U^{(2)} = U_{\text{val}}^{(2)}$. Thus we obtain the following results for the second-order π^{13}C optical potentials: $V_{\pi^\pm {}^{13}\text{C}}^{(2)} = W^{(2)} \mp U^{(2)}$; or conversely,

$$W^{(2)} = \tfrac{1}{2}(V_{\pi^- {}^{13}\text{C}}^{(2)} + V_{\pi^+ {}^{13}\text{C}}^{(2)}) \tag{3.6}$$

and

$$U^{(2)} = \tfrac{1}{2}(V_{\pi^- {}^{13}\text{C}}^{(2)} - V_{\pi^+ {}^{13}\text{C}}^{(2)}) . \tag{3.7}$$

We now proceed to determine $W^{(2)}$ and $U^{(2)}$ by considering those reaction mechanisms that

represent the dominant contribution of two-nucleon processes in the calculation of second-order potentials. We first consider the true absorption of pions by two nucleons. Contributions of this reaction mechansim (denoted as mechanism A) to the second-order pion-nucleus potential are illustrated by Fig. 1(a). In Fig. 1(b), we show a microscopic model for the true pion absorption process ($\pi NN \to NN$). In this model the pion is scattered from a first nucleon and is then absorbed by a second nucleon. The two nucleons may or may not be strongly correlated. This two-step absorption mechansim represents the dominant mode for pion absorption in the (3,3) resonance region and has been extensively employed in many theoretical calculations.[30] In isospin space, the absorption amplitude can be labeled by A_{TI}, which corresponds to the initial isospin T and to the final isospin I of the two nucleons. [The quantity I is also equal to the total isospin of the initial (πNN) three-body system]. There are three independent amplitudes[31]: A_{10}, A_{01}, and A_{11}. Applying standard angular momentum algebra to the analysis of the two-step mechanism of Fig. 1(b), we obtain:

$$A_{TI} = \sum_{I_s} g_{I_s I}(-1)^I [2I_s+1)(2T+1)]^{1/2} \begin{Bmatrix} 1 & \frac{1}{2} & I_s \\ \frac{1}{2} & I & T \end{Bmatrix}, \tag{3.8}$$

where

$$g_{I_s I} = -i\sqrt{3}(-1)^{3/2+I_s}[2(2I_s+1)]^{1/2} f_{(I_s)} \begin{Bmatrix} 1 & \frac{1}{2} & I_s \\ I & \frac{1}{2} & \frac{1}{2} \end{Bmatrix}. \tag{3.9}$$

Here the factor $-i\sqrt{3}$ arises from the πNN vertex. The quantity $f_{(I_s)}$ is the πN scattering amplitude in the channel of isospin I_s.[32] Detailed evaluation yields:

$$A_{10} = -i\sqrt{3} f_{(1/2)}, \tag{3.10a}$$

$$A_{01} = \tfrac{1}{3}(-4 f_{(3/2)} + f_{(1/2)}), \tag{3.10b}$$

and

$$A_{11} = \frac{-\sqrt{2}}{3}(2 f_{(3/2)} + f_{(1/2)}). \tag{3.10c}$$

The scattering amplitude of a pion in an initial isopin state $|1,\lambda\rangle$ by two nucleons in an isopin state $|T,m\rangle$, via mechanism A, to a final isopin state $|1,\lambda'\rangle$ with the two nucleons left in a final isopin state $|T',m'\rangle$, is therefore proportional to

$$S_A^{\lambda' T' m', \lambda T m} = \sum_I C^{1TI}_{\lambda' m' M} C^{1TI}_{\lambda m M} A_{TI} A^{\dagger}_{T'I}. \tag{3.11}$$

Here, $\lambda = 1, 0, -1$ represent, respectively, the value of the third isopin component of π^+, π^0, π^-. Further, we have the relation $A^{\dagger}_{T'I} = (A_{T'I})^*$. If the charge state of the pion is unchanged ($\lambda' = \lambda$), only transitions with $T = T'$ and $m = m'$ are allowed for nuclei with closed shells. Equation (3.11) thus reduces to

$$S_A^{\lambda T m} \equiv \sum_I \begin{pmatrix} 1 & T & I \\ \lambda & m & \lambda+m \end{pmatrix}^2 |A_{TI}|^2 \tag{3.12}$$

$$= \delta_{T,0}\delta_{m,0}|A_{01}|^2 + \delta_{T,1}[\tfrac{1}{3}\delta_{\lambda,-m}|A_{10}|^2 + \tfrac{1}{4}(2+m\lambda)(1-m\lambda)(1-\delta_{m,0}) + \frac{\lambda^2}{2}\delta_{m,0}|A_{11}|^2], \tag{3.13}$$

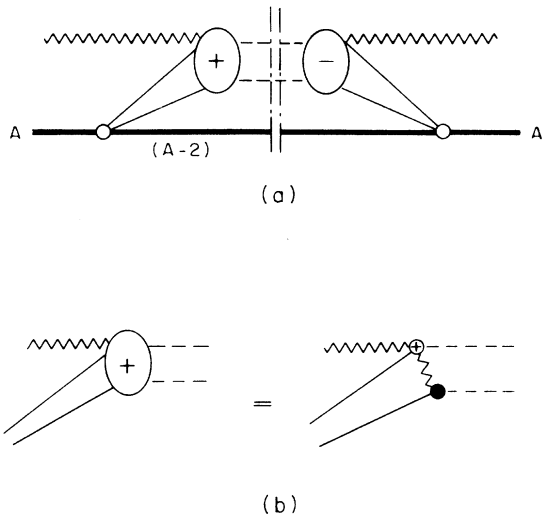

FIG. 1. (a) Diagrammatic representation of the contribution of the true pion absorption process to the second-order pion-nucleus interaction. Pions and target nucleons are represented by wavy and simple solid lines. The dashed lines represent nucleons in states that are unoccupied in the target ground state. The vertical lines indicate that the spectral decomposition of Eq. (2.12) has been used. The heavy solid lines denote nuclei containing A or A-2 particles. The small open circles denote nuclear vertex functions; the large open circles containing the plus and minus signs are, respectively, the pion absorption and production amplitudes. (b) Diagrammatic representation of the two-step model for the pion absorption amplitude of (a). The filled circle is the πNN vertex function; the open circle with the plus sign is the πN scattering amplitude.

where the subscript A refers to reaction mechanism A. When the pion is scattered from a valence nucleon-core nucleon pair, $T \neq T'$ transitions are allowed. However, one must have $m' = m$ when $\lambda' = \lambda$. The only possible values for m' and m are thus $m' = m = 0$. That is, $T' \neq T$ transitions can take place only for a valence-core nucleon pair consisting of a proton and a neutron. Owing to the antisymmetrization of the wave function of two nucleons, a change in the total isospin of the two nucleons is necessarily accompanied by a corresponding change in the spin-space part of the two nucleon wave functions. The contribution from $T' \neq T$ transitions is therefore much smaller than that from $T' = T$ transitions. We define, therefore, a strength function

$$S_A \equiv \sum_T S_A^{\lambda T m} \tag{3.14}$$

which represents the sum of all $T' = T$ contributions to the scattering of the pion from a nucleon pair. Expressions for S_A due to various combinations of nucleon pairs are given in Table I. We have used the notations $\pi[np]$, $\pi[nn]$, and $\pi[pp]$ to imply the summation over all T values of the two-particle isospin states of definite symmetry, as required by Eq. (3.14). Hence in this notation, we have $S_A(\pi[np]) = S_A(\pi[pn])$. We shall also use the notation (np), (nn), (pn), and (pp) to indicate the physical combinations of two nucleons, which do not necessarily have a definite isospin value. For example, $|(np)\rangle = (|T=1\rangle - |T=0\rangle)/\sqrt{2}$ and $|(pn)\rangle = (|T=1\rangle + |T=0\rangle)/\sqrt{2}$, etc. In this latter notation, the (np) and (pn) are counted as two distinct combinations. Since (nn) and (pp) are in a pure isospin state while (np) and (pn) are not, we have $S_A(\pi(nn)) = S_A(\pi[nn])$, while $S_A(\pi(np)) = S_A(\pi[np])/2$, etc. We will also use the subscript v or c to denote whether a valence or a core particle is involved. When the symbol N is used, it implies a sum over the two charge states of the nucleon N. For example, (NN) is equivalent to four combinations: (nn), (np), (pn), and (pp). Employing these notations, we find from Table I that the contribution due to all four possible charge states associated with a core nucleon pair is

$$S_A(\pi(N_c N_c)) = |A_{01}|^2 + |A_{11}|^2 + |A_{10}|^2. \tag{3.15}$$

There are $A_c(A_c - 1)/2$ charge states for A_c core nucleons. To each of these states one can associate an average strength function $\bar{S}_A = S_A(\pi(N_c N_c))/4$. For the valence-core nucleon pair, the strength functions due to π^+ and π^- differ from each other. We have, for example:

$$\begin{aligned} S_A(\pi^+(n_v N_c)) &\equiv S_A(\pi^+[n_v n_c]) + \tfrac{1}{2} S_A(\pi^+[n_v p_c]) \\ &= \tfrac{1}{2}|A_{01}|^2 + |A_{11}|^2 + |A_{10}|^2, \end{aligned} \tag{3.16}$$

and

$$\begin{aligned} S_A(\pi^-(n_v N_c)) &= S_A(\pi^-[n_v n_c]) + \tfrac{1}{2} S_A(\pi^-[n_v p_c]) \\ &= \tfrac{1}{2}|A_{01}|^2 + \tfrac{1}{4}|A_{11}|^2. \end{aligned} \tag{3.17}$$

There are $\mathfrak{N}_v A_c$ charge states, with $\mathfrak{N}_v$ being the number of valence neutrons. ($\mathfrak{N}_v = 1$ for ^{13}C.) Each of these charge states is associated with an average strength function $\bar{S}_A = S_A(\pi^+(n_v N_c))/2$, since each $(n_v N_c)$ is equivalent to two charge states. The total contribution to the $\pi^{\pm}$ ^{13}C system is therefore given by:

$$S_{\pi^\pm\,^{13}\mathrm{C}} = \tfrac{1}{8} A_c(A_c - 1) S_A(\pi(N_c N_c)) + \tfrac{1}{2}\mathfrak{N}_v A_c S_A(\pi^\pm(n_v N_c)). \tag{3.18}$$

Similarly, the corresponding quantity for the pion-^{12}C system is

$$S_{\pi\,^{12}\mathrm{C}} = \tfrac{1}{8} A_c(A_c - 1) S_A(\pi(N_c N_c)). \tag{3.19}$$

Since the difference between the nucleon density distributions in ^{12}C and ^{13}C is small,[33] we neglect the difference between the single-particle shell model wave functions used in these two neighboring nuclei. The second-order optical potentials for π ^{13}C systems are then determined with the relation

$$V_{\pi^\pm\,^{13}\mathrm{C}}^{(2)} = \eta_\pm(E) V_{\pi\,^{12}\mathrm{C}}^{(2)}, \tag{3.20}$$

where $\eta_\pm(E)$ is an energy-dependent scaling factor defined by

$$\eta_\pm(E) = \frac{S_{\pi^\pm\,^{13}\mathrm{C}}}{S_{\pi\,^{12}\mathrm{C}}} = 1 + \frac{4\mathfrak{N}_v}{A_c - 1} \frac{S_A(\pi^\pm(n_v N_c))}{S_A(\pi(N_c N_c))}. \tag{3.21}$$

Equations (3.20) and (3.21) represent our scaling method. The isoscalar and isovector part of the interaction can therefore be obtained by using Eqs. (3.4) and (3.5). The results are:

$$W_0^{(2)} = \eta_W(E) V_{\pi\,^{12}\mathrm{C}}^{(2)}, \tag{3.22}$$

and

$$U_0^{(2)} = \eta_U(E) V_{\pi\,^{12}\mathrm{C}}^{(2)}, \tag{3.23}$$

TABLE I. Expressions for strength functions S_A.

Systems	M	m	S_A
$\pi^0[pp]$	1	1	$\frac{1}{2}\lvert A_{11}\rvert^2$
$\pi^+[np]$	1	0	$\lvert A_{01}\rvert^2 + \frac{1}{2}\lvert A_{11}\rvert^2$
$\pi^-[pp]$	0	1	$\frac{1}{2}\lvert A_{11}\rvert^2 + \frac{1}{3}\lvert A_{10}\rvert^2$
$\pi^0[np]$	0	0	$\lvert A_{01}\rvert^2 + \frac{1}{3}\lvert A_{10}\rvert^2$
$\pi^+[nn]$	0	−1	$\frac{1}{2}\lvert A_{11}\rvert^2 + \frac{1}{3}\lvert A_{10}\rvert^2$
$\pi^-[np]$	−1	0	$\lvert A_{01}\rvert^2 + \frac{1}{2}\lvert A_{11}\rvert^2$
$\pi^0[nn]$	−1	−1	$\frac{1}{2}\lvert A_{11}\rvert^2$

where the scaling factors η_W and η_U are defined, respectively, by $\eta_W = (\eta_+ + \eta_-)/2$ and $\eta_U = (\eta_- - \eta_+)/2$. Our calculations show that the values of $\eta_W(E)$ are $\simeq 1.18$, being nearly independent of energy. The values of $\eta_U(E)$ are given in Table III.

In a similar way, we consider the two-nucleon mechanism associated with the scattering of pions from a correlated pair of nucleons. This reaction mechanism, denoted as B, is shown in Fig. 2, where the open circles with the plus and minus signs denote the πN amplitude and its complex conjugate. As emphasized in Sec. II, the presence of the product of the πN scattering amplitude and its complex conjugate represents the main difference between our approach and the usual multiple-scattering approach to the calculation of the second-order optical potential. Owing to the presence of the pion in the intermediate states in Fig. 2, there are five independent isospin amplitudes describing the $\pi NN \to \pi NN$ scattering. These amplitudes can be labeled by $M^I_{T''T}$, with T'' and T being the final and initial isospin of the two nucleons, and I being the total isospin of the πNN system. Standard angular momentum algebra gives the following results:

$$M^I_{T''T} = \sum_{I_s} (2I_s+1)[(2T''+1)(2T+1)]^{1/2} \times f_{(I_s)} \begin{Bmatrix} 1 & \frac{1}{2} & I_s \\ \frac{1}{2} & I & T'' \end{Bmatrix} \begin{Bmatrix} 1 & \frac{1}{2} & I_s \\ \frac{1}{2} & I & T \end{Bmatrix} \tag{3.24}$$

and

$$(M^\dagger)^I_{TT''} = (-1)^{T+T''}(M^I_{T''T})^*. \tag{3.25}$$

Detailed calculations show that

$$M^0_{11} = f_{(1/2)}, \tag{3.26}$$

$$M^1_{00} = \tfrac{2}{3} f_{(3/2)} + \tfrac{1}{3} f_{(1/2)}, \tag{3.27}$$

$$M^1_{10} = \frac{\sqrt{2}}{3}(f_{(3/2)} - f_{(1/2)}), \tag{3.28}$$

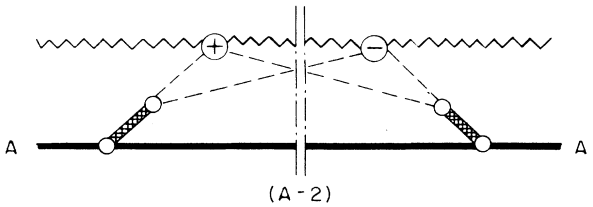

FIG. 2. Representation of the contribution to the second-order pion-nucleus interaction arising from pion scattering from a correlated pair. The correlations are indicated by cross-hatched double lines. The open circles with the plus and minus signs denote the πN amplitude and its complex conjugate. The other circles and lines have the same meaning as in Fig. 1.

$$M^1_{11} = \tfrac{1}{3} f_{(3/2)} + \tfrac{2}{3} f_{(1/2)}, \tag{3.29}$$

and

$$M^2_{11} = f_{(3/2)}. \tag{3.30}$$

In analogy to Eqs. (3.11) and (3.12), we define, respectively,

$$S_B^{\lambda' T' m', \lambda T m} = \sum_I C^{1T'I}_{\lambda' m' M} C^{1TI}_{\lambda m M} V^I_{T'T} \tag{3.31}$$

and

$$S_B^{\lambda T m} = \sum_I \begin{pmatrix} 1 & T & I \\ C_\lambda & m & \lambda+m \end{pmatrix}^2 V^I_{TT}, \tag{3.32}$$

where

$$V^I_{TT} \equiv \sum_{T''} M^I_{TT''}(M^\dagger)^I_{T''T}. \tag{3.33}$$

The strength function in this model is then defined as

$$S_B \equiv \sum_T S_B^{\lambda T m}. \tag{3.34}$$

Here the subscript B stands for the reaction mechanism B. Expressions for S_B are presented in Table II. Using considerations similar to those leading to Eqs. (3.15)–(3.17), we obtain

$$S_B(\pi(N_c N_c)) = \tfrac{5}{3}V^2_{11} + V^1_{11} + V^1_{00} + \tfrac{1}{3}V^0_{11}, \tag{3.35}$$

$$S_B(\pi(n_v N_c)) = \tfrac{5}{12}V^2_{11} + \tfrac{3}{4}V^1_{11} + \tfrac{1}{2}V^1_{00} + \tfrac{1}{3}V^0_{11}, \tag{3.36}$$

and

$$S_B(\pi(n_v N_c)) = \tfrac{5}{4}V^2_{11} + \tfrac{1}{4}V^1_{11} + \tfrac{1}{2}V^1_{00}. \tag{3.37}$$

The scaling factors $\eta_\pm(E)$ are defined through the use of equations similar to Eqs. (3.18)–(3.23). We find that $\eta_W(E) \simeq 1.18$, being again independent of energy. The values of $\eta_U(E)$ are given in Table III.

Let us denote the scaling factors η_U determined from the reaction mechanisms A and B, respec-

TABLE II. Expressions for strength functions S_B.

Systems	M	m	S_B
$\pi^+[pp]$	2	1	V^2_{11}
$\pi^0[pp]$	1	1	$\frac{1}{2}V^2_{11} + \frac{1}{2}V^1_{11}$
$\pi^-[pp]$	0	1	$\frac{1}{6}V^2_{11} + \frac{1}{2}V^1_{11} + \frac{1}{3}V^0_{11}$
$\pi^+[np]$	1	0	$\frac{1}{2}V^2_{11} + \frac{1}{2}V^1_{11} + V^1_{00}$
$\pi^0[np]$	0	0	$\frac{2}{3}V^2_{11} + V^1_{00} + \frac{1}{3}V^0_{11}$
$\pi^-[np]$	−1	0	$\frac{1}{2}V^2_{11} + \frac{1}{2}V^1_{11} + V^1_{00}$
$\pi^+[nn]$	0	−1	$\frac{1}{6}V^2_{11} + \frac{1}{2}V^1_{11} + \frac{1}{3}V^0_{11}$
$\pi^0[nn]$	−1	−1	$\frac{1}{2}V^2_{11} + \frac{1}{2}V^1_{11}$
$\pi^-[nn]$	−2	−1	V^2_{11}

tively, by η_U^A and η_U^B. We see from Table III that η_U^A and η_U^B have opposite signs at most energies. This feature is easily understood. In the true absorption mechanism, the absorption of π^- takes place on an n-p pair or on a p-p pair, while the absorption of π^+ requires the presence of an n-p pair or an n-n pair. In ^{13}C, there are fewer p-p pairs than n-n pairs, and consequently reaction mechanism A leads to $\eta_- < \eta_+$ and $\eta_U^A < 0$. On the other hand, for the reaction mechanism B the strength is governed by the pion-nucleus scattering processes. In the (3, 3) resonance region, $\pi^- n$ scattering is stronger than $\pi^+ n$ scattering. This basic feature of πN scattering is reflected in the relative strengths between scattering from various pairs, as shown in Table II. Again, since $N > Z$ in ^{13}C, there are more pairs favoring π^- scattering than π^+ scattering. Consequently, reaction mechanism B leads to $\eta_- > \eta_+$ and $\eta_U^B > 0$.

An inspection of Figs. 1 and 2 shows that the intermediate states in the two reaction mechanisms discussed above are orthogonal. In mechanism A, there is no pion in the intermediate state, whereas in mechanism B a pion is present. When both reaction mechanisms are contributing to the second-order pion-nucleus interaction, the effective scaling factor should therefore be a combination of η_U^A and η_U^B. We propose to write

$$\eta_U(E) = [1 - X(E)]\eta_U^A(E) + X(E)\eta_U^B(E). \tag{3.38}$$

In Eq. (3.38) the energy-dependent quantity $X(E)$ defines the degree of mixing of two reaction mechanisms, and $X(E)$ can be determined by comparing the experimental excitation function with theoretical SCE cross sections calculated with $\eta_U(E)$ of Eq. (3.38). Since η_U^A and η_U^B have opposite signs, it is possible that for a given energy E, η_U may vanish. This implies that at this energy, the mixing parameter is given by

$$X(E) = -\eta_U^A(E)/[\eta_U^B(E) - \eta_U^A(E)]. \tag{3.39}$$

Before concluding this section, we discuss the effect of neglect of $T' \neq T$ terms in Eqs. (3.14) and (3.21). We find that the inclusion of these terms has only a small effect on the calculated cross sections. By way of clarification, we note from the preceding discussion that only $(n_v p_c)$ pairs contribute to $T' \neq T$ transitions, while both $(n_v p_c)$ and $(n_v n_c)$ pairs contribute to $T' = T$ transitions. Taking into account this feature, we have calculated $S^{\lambda T'm, \lambda Tm}$ and the change in η_U due to all allowed $T' \neq T$ transitions using Eqs. (3.11), (3.31), and (3.21). Owing to the model-dependence feature of S and η_U, the change in η_U^B is much smaller than the change in η_U^A. For η_U^A, the $T' \neq T$ transitions cause a modification of ~ 20% of the values given in Table III. However, the overall change in the calculated cross sections is much less than 20%, since the overlap between the initial and final nuclear wave functions in a $T' \neq T$ transition is much less than that in a $T' = T$ transition. If we let $V^{(2)}_{\lambda T'm, \lambda Tm}$ denote the contribution to the second-order potential arising from a given $(Tm) \to (T'm)$ transition and a pion in the charge state λ, and if we factor out the πNN interactions from the rest of the evaluation of the reaction diagrams shown in Figs. 1(a) and 2(a), we obtain[3] $\langle \vec{k}' | V^{(2)}_{\lambda T'm, \lambda Tm}(E) | \vec{k} \rangle \propto S^{\lambda T'm, \lambda Tm}(E) I_{T'T}(\vec{q})$, where $I_{T'T}(\vec{q})$ describes the overlap between the initial and final nuclear wave functions, and $\vec{q}$ is the momentum transfer. Since the total two-nucleon wave function is antisymmetric, a change of the total isopin of the system must be accompanied by a change of the symmetry of the spin-space part of the wave function. For example, if $T = 1$, then the isospin part of the two-nucleon wave function is symmetric and the spin-space part is antisymmetric. If $T = 0$, then the isospin part of the wave function is antisymmetric and the spin-space part is symmetric. The change of symmetry of the spin-space parts of the wave functions in a $T' \neq T$ transition reduces considerably the value of the overlap integral $I_{T'T}$. We estimated this reduction effect by assuming that the total spin of the two-nucleon system was unchanged during the interaction. [This simplification will introduce only a small error as a result of the weak πN spin-flip interaction in the (3, 3) resonance region.] Single-particle harmonic oscillator wave functions were used to construct the two-nucleon wave functions with definite symmetry.[34] Our estimate has shown that the average value of the overlap integrals for $T' \neq T$ is about one third of that for $T' = T$. The overall effect of $T' \neq T$ transitions on the second-order potential is therefore $20\% \times \frac{1}{3} \simeq 7\%$. Furthermore, because of the presence of the first-order SCE potential this 7% change in the second-order SCE potential has caused only ~3% change in the calculated SCE cross sections.

TABLE III. Values of η_U as function of pion energies.

T_π (MeV)	η_U^A	η_U^B
30	−0.152	−0.0950
50	−0.0812	0.0098
80	−0.0447	0.0547
100	−0.0374	0.0690
120	−0.0342	0.0775
150	−0.0320	0.0846
162	−0.0316	0.0862
180	−0.0309	0.0886
200	−0.0306	0.0904
230	−0.0301	0.0928
260	−0.0297	0.0957

IV. RESULTS AND DISCUSSION

Using the procedure outlined in the previous sections, we have calculated the excitation function of the SCE reaction $^{13}C(\pi^+, \pi^0)^{13}N(g.s.)$. The results are presented in Fig. 3. If we assume that only the true pion absorption mechanism contributes to the second-order potentials, we obtain curve A. Similarly, curve B corresponds to the situation in which the contribution to the second-order potentials comes only from the two-nucleon process involving the scattering of pions from nucleon pairs. The excitation function obtained in the limit $\eta_U = 0$ is represented by the dashed curve in Fig. 3. For comparison, we also show the result when the second-order interaction is entirely omitted from the theory (dash-dotted curve). This last result is, of course, not realistic since we know from the analysis of elastic scattering data that two-nucleon processes are very important.[4] In Fig. 3, with the exception of the dash-dotted curve, all other theoretical excitation functions exhibit a minimum at pion energy near 150 MeV. In Fig. 4, we compare theoretical results with the experimental angular distribution of Ref. 19. The prediction for the SCE differentical cross sections at 180 MeV is presented in Fig. 5. In both Figs. 4 and 5, we note the first minimum occurs at $\theta_{c.m.} \simeq 36°$. This minimum is related to the first minimum in the nuclear form factor of the valence neutron. It is worth mentioning that if only the first-order theory was used, one would obtain differential cross sec-

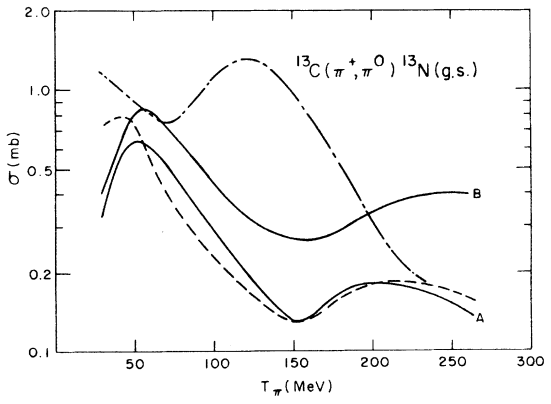

FIG. 3. Theoretical excitation functions for the SCE reaction $^{13}C(\pi^+, \pi^0)^{13}N(g.s.)$. Curve A corresponds to the situation in which only the true absorption processes contribute to $V^{(2)}$. Results calculated with the assumption that $V^{(2)}$ is due solely to pion scattering from correlated pairs are represented by curve B. The dashed curve represents the excitation function calculated in the limit $\eta_U = 0$. The dot-dash curve indicates theoretical results when only the first-order interaction is used.

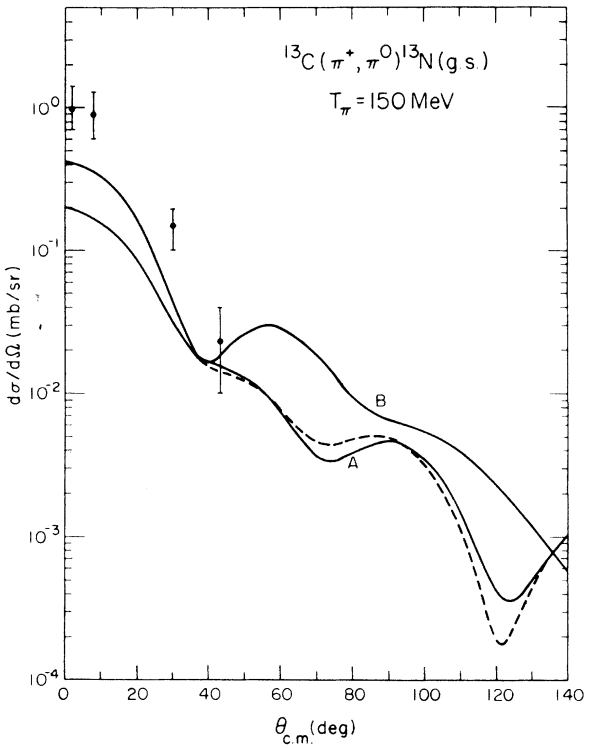

FIG. 4. Theoretical results for the angular distributions for $^{13}C(\pi^+, \pi^0)^{13}N(g.s.)$ at 150 MeV. Data are from Ref. 19. Notation is the same as for Fig. 3.

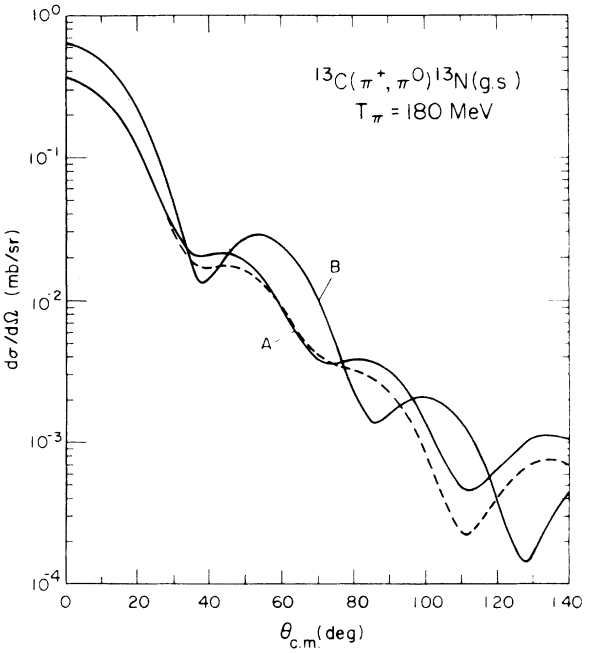

FIG. 5. Predictions for differential cross sections for $^{13}C(\pi^+, \pi^0)^{13}N(g.s.)$ at 180 MeV. Notation is the same as for Fig. 3.

tions having first minima at $\theta_{c.m.} \simeq 45°$. Consequently, the inclusion of the second-order interaction has effects equivalent to those produced by increasing the rms radius of the valence neutron distribution. This feature has also been observed in our previous studies of pion-nucleus elastic scattering.[4] Consequently, we believe that in the absence of a reliable calculation of the second-order pion-nucleus strong interaction, SCE reactions do not provide a simple measure of the neutron distribution. Indeed, we have also investigated the role of the valence neutron distribution in ^{13}C, and we have found that with a reasonable variation of this distribution the effect on the calculated excitation function is very small.

It is of interest to compare the theoretical elastic scattering differential cross sections, obtained from this work, with experimental data.[35,36] The comparisons are shown in Fig. 6 for π^+-^{13}C and π^--^{13}C elastic scattering at 180 MeV and in Fig. 7 for π^+-^{13}C elastic scattering at 50 MeV. In all these calculations, we use the microscopic first-order potential described in Sec. II and the second-order potential determined from scaling the phenomenological pion-^{12}C second-order optical potential.[4] Since no new adjustable parameter has been introduced in this calculation, we are greatly encouraged by the good agreement obtained between our theory and the data.

Inspection of Figs. 3–7 reveals that while theoretical elastic differential cross sections are rather insensitive to the dynamics of two-nucleon processes, *calculated excitation functions of the SCE reaction depend strongly on the nature of the two-nucleon processes*. The integrated cross sections calculated with several values of the mixing parameter X are shown in Table IV. The cross sections are quite sensitive to the value of X, especially for $X \geq 0.50$. Consequently, SCE represents a useful tool to study pion-nucleus dynamics. For example, the quantity $X(E)$ may be determined in certain cases by comparing theoretical results with data. The kind of analysis proposed here will allow us to obtain information about the energy-dependence of true pion absorption and to supplement various microscopic calculations of pion-two-nucleon processes.

Since the second-order pion-^{12}C optical potential does not have a spin-flip term, the scaling method of Sec. III does not allow us to determine $W_s^{(2)}$ and $U_s^{(2)}$. However, our calculations do include the first-order spin-flip terms $W_s^{(1)}$ and $U_s^{(1)}$. Contributions to the excitation function from the first-order spin-flip terms is negligible for pion energy greater than 100 MeV and becomes quite important at low energies ($\lesssim$ 80 MeV). Since contributions from the second-order spin-flip potentials are

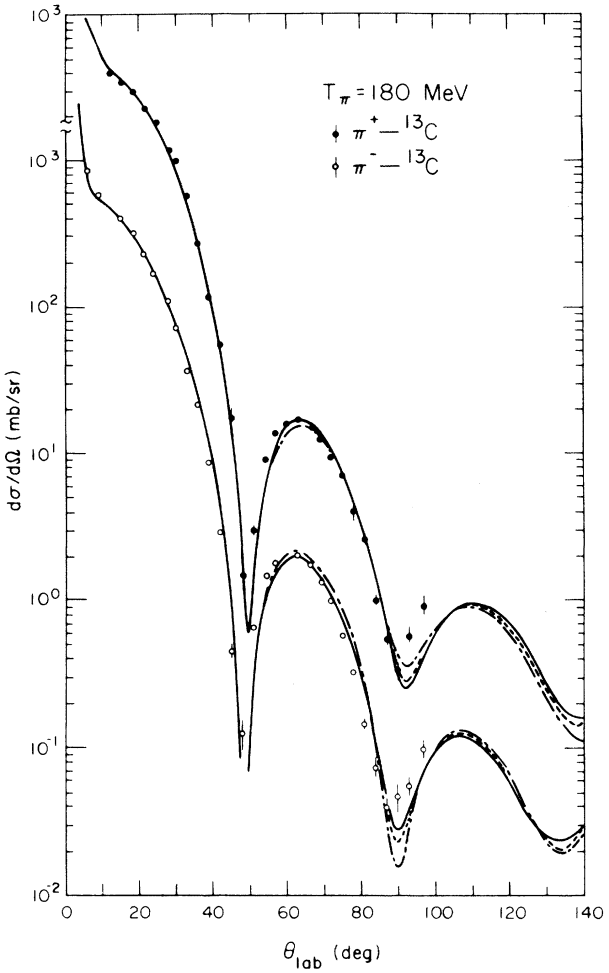

FIG. 6. Calculated differential cross sections for π^+ ^{13}C and π^- ^{13}C elastic scattering at 180 MeV. Data are taken from Ref. 32. The solid curves correspond to the situation in which only the true pion absorption processes contributes to $V^{(2)}$. Results calculated with the assumption that $V^{(2)}$ is due to pion scattering from correlated pairs are represented by the dot-dash curves. The dashed curves represent theoretical results calculated in the limit $\eta_U = 0$.

expected to be much less important than those from $W_s^{(1)}$ and $U_s^{(1)}$, the analysis proposed in this work should be reliable for pion energies greater than 100 MeV.

The present analysis also indicates that although it is possible to have $\eta_U^{(2)}$ equal to zero, it is not possible to have $\eta_W^{(2)}$ equal to zero. Translated into the distorted-wave formalism, this means that the calculations can be carried out with omission of the second-order direct interaction and inclusion of the second-order distorting potentials in the calculation of distortions. In this case, we obtain very small SCE cross sections. In fact,

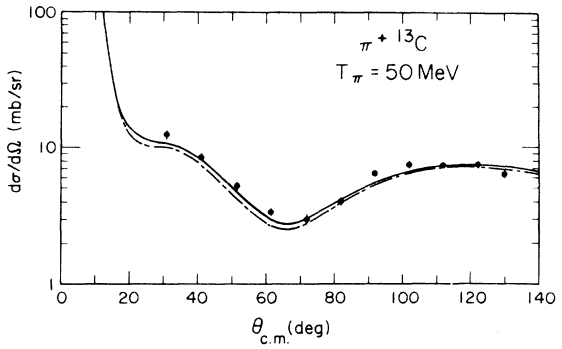

FIG. 7. Calculated differential cross sections for $\pi^+ {}^{13}C$ elastic scattering at 50 MeV. Data are taken from Ref. 33. Notation is the same as for Fig. 6.

we cannot omit the second-order distorting potentials in the calculation of distortions while keeping second-order potentials in the direct interaction. (In general, this latter procedure gives higher SCE cross sections.)

In summary, we have presented a coupled-channel approach to single charge exchange reactions. When SCE reactions leading to an isobaric analog state are considered, one obtains a system of two coupled equations in which the diagonal matrix elements of the effective interaction can be identified with second-order pion-nucleus optical potentials. The off diagonal part of this effective interaction is responsible for charge exchange. Various spin and isospin terms of the effective interaction

TABLE IV. Calculated integrated cross sections (in mb) for the $^{13}C(\pi^+, \pi^0)^{13}N$(g.s.) SCE reaction as a function of X.

T_π (MeV)	$X=0.$	$X=0.25$	$X=0.50$	$X=0.75$	$X=1.00$
120	0.20	0.17	0.18	0.22	0.31
180	0.17	0.16	0.18	0.22	0.29
230	0.17	0.18	0.21	0.28	0.39

can be determined from phenomenological optical potentials of neighboring nuclei by use of isospin symmetry properties. In considering microscopic models for the construction of the effective interaction, we have used a unitary theory of optical potentials for strongly interacting particles.[21] This approach facilitates the physical interpretation of the theoretical results and does not lead to spurious enchancement of cross sections. From the study of the pion-^{13}C system, we find that theoretical results for the SCE reaction leading to the IAS are quite sensitive to two-nucleon processes. This indicates that SCE reactions leading to the IAS offer a useful tool for probing pion-nucleus dynamics. Finally, the method developed here can be generalized to study SCE reactions on nuclei with any spin and isospin and to study double charge exchange reactions.

This work was performed under the auspices of the U. S. Department of Energy.

[1]J. E. Spencer, in *Proceedings of the Seventh International Conference on High-Energy Physics and Nuclear Structure, Zurich 1977*, edited by M. P. Locher (Birkhauser, Basel and Stuttgart, 1977, pp. 153-172, also references contained therein.

[2]Detailed account of experimental and theoretical studies can be found in LAMPF Workshop on Pion Single Charge Exchange, 1979, LASL Report No. LA-7892-C, (unpublished).

[3]L. C. Liu and C. M. Shakin, Phys. Rev. C 16, 333 (1977).

[4]L. C. Liu, Phys. Rev. C 17, 1787 (1978); L. C. Liu and C. M. Shakin, *ibid.* 19, 129 (1979); R. S. Bhalerao, L. C. Liu, and C. M. Shakin, *ibid.* 21, 1903 (1980).

[5]K. Stricker, H. McManus, and J. A. Carr, Phys. Rev. C 19, 929 (1979); R. H. Landau and A. W. Thomas, Nucl. Phys. A302, 461 (1978).

[6]L. Celenza, L. C. Liu, and C. M. Shakin, Phys. Rev. C 11, 1593 (1975); 12, 721 (1975) (E).

[7]Calculations similar to ours are reported in J. P. Maillet, J. P. Dedonder, and C. Schmitt, Nucl. Phys. A316, 267 (1979).

[8]Y. Shamai, J. Alster, D. Ashery, S. Cochavi, M. A. Moinester, A. I. Yavin, E. D. Arthur, and D. M. Drake, Phys. Rev. Lett. 36, 82 (1976).

[9]M. Zaider *et al.*, in *Proceedings of the Fifth International Conference on High-Energy Physics and Nuclear Structure*, edited by G. Tibell (North-Holland, Amsterdam, 1973), p. 129.

[10]W. R. Gibbs, in *Theoretical Methods in Medium-Energy and Heavy Ion Physics*, edited by K. W. McVoy and W. A. Friedman (Plenum, New York, 1978), p. 503; L. C. Liu and V. Franco, Phys. Lett. 61B, 454 (1976); A. Reitan, Nucl. Phys. B68, 387 (1974).

[11]W. R. Gibbs, B. F. Gibson, A. T. Hess, and G. J. Stephenson, Jr., Phys. Rev. Lett. 36, 85 (1976); D. Tow and J. M. Eisenberg, Nucl. Phys. A237, 441 (1975).

[12]S. Chakravarti, Phys. Lett. 90B, 350 (1980); T.-S. H. Lee and D. Kurath, Phys. Rev. C 21, 293 (1980).

[13]A relatively smooth energy-dependence of the cross sections has been obtained in a Glauber type calculation by E. Oset and D. Strottman, who made use of modified pion-nucleon amplitude. (See LASL Report No. LA-UR-80-627, 1980 (unpublished).

[14]A. N. Saharia and R. M. Woloshyn, Phys. Rev. C 21, 1111 (1980).

[15]E. J. Moniz and M. Toyama, MIT report (unpublished).

[16]R. H. Landau and A. W. Thomas, Phys. Lett. 88B,

226 (1979).
[17]G. J. Stephenson, Jr., Wayne Polyzou, and W. R. Gibbs, Bull. Amer. Phys. Soc. 25, 606 (1980).
[18]R. E. Anderson, J. J. Kraushaar, E. Rost, and D. A. Sparrow, University of Colorado 1976 Report (unpublished).
[19]J. D. Bowman, Nucl. Phys. A335, 375 (1980).
[20]Experiments are being prepared at LAMPF by the Users's groups of the π^0 spectrometer and, independently, by the LAMPF nuclear chemistry group. The latter group will perform activation measurements on thin targets.
[21]L. C. Liu and C. M. Shakin, Phys. Rev. C 20, 2339 (1979).
[22]J. Warzawski, A. Gal, and J. M. Eisenberg, Nucl. Phys. A294, 321 (1978).
[23]H. Garcilazo, Nucl. Phys. A302, 493 (1978).
[24]A. M. Lane, Nucl. Phys. 35, 676 (1962).
[25]C. Mahaux and H. A. Weidenmuller, Nucl. Phys. 89, 33 (1966).
[26]D. Robson, Phys. Rev. 137, B535 (1965).
[27]C. M. Vincent and S. C. Phatak, Phys. Rev. C 10, 391 (1974).
[28]J. Heisenberg, J. S. McCarthy, and I. Sick, Nucl. Phys. A157, 435 (1970).
[29]L. C. Liu and C. M. Shakin, Nuovo Cimento 53A, 142 (1979).
[30]K. Breuckner, Phys. Rev. 98, 769 (1955); M. Ericson and T. E. O. Ericson, Ann. Phys. (N.Y.) 36, 323 (1966); D. Koltun, Phys. Rev. 162, 963 (1967); F. Hochenberg, J. Hufner, and H. J. Pirner, Phys. Lett. 66B, 425 (1977).
[31]E. Fermi, Nuovo Cimento Suppl. 2, 17 (1955).
[32]B. H. Bransden and R. G. Moorhouse, *The Pion-Nucleon System* (Princeton University Press, Princeton, 1973), pp. 45–47.
[33]The differences between the rms radii of the protons and those of the neutrons in ^{13}C and in ^{12}C are, respectively, ~ 0.1 and ~ 0.04 fm. See, respectively: H. R. Collard, L. R. B. Elton, and R. Hofstadter, in *Nuclear Radii*, Landolt-Bornstein New Series, edited by H. Schopper (Springer, Berlin-Heidelberg-New York, 1967), Vol. 2; J. Alster, Los Alamos Scientific Laboratory Report No. LA-8303-C, 1980.
[34]A. de-Shalit and I. Talmi, in *Nuclear Shell Theory* (Academic, New York, 1963), p. 192.
[35]E. Schwarz, J.-P. Egger, F. Goetz, P. Gretillat, and C. Lunke, Phys. Lett. 43B, 1578 (1979).
[36]S. A. Dytman, J. F. Amann, P. D. Barnes, J. N. Craig, K. G. R. Doss, R. A. Eisenstein, J. D. Sherman, W. R. Wharton, G. R. Burleson, S. L. Verbeck, R. J. Peterson, and H. A. Thiessen, Phys. Rev. C 18, 2316 (1978).